Performance of up-flow microbial fuel cells in synthetic landfill leachate treatment explained by discrete effects of hydraulic retention time and initial substrate concentration

Songyot Mongkulphit[1] and Petch Pengchai[2*]

[1] Faculty of Engineering, Northeastern University, Khon Kaen 40000, Thailand
[2] Faculty of Engineering, Mahasarakham University, Mahasarakham 44150, Thailand

ABSTRACT

This study aimed to explain the performance of microbial fuel cells (MFCs) using hydraulic retention time (HRT) and initial substrate concentration (C_0) independently. In two experiments, synthetic landfill leachate (35 L/d) was applied to up-flow MFCs at 6 different HRTs and 6 different C_0s. Water quality parameters such as chemical oxygen demand (COD) and nutrient content were analyzed during the process. The up-flow MFCs produced 1–80 mW/m^2 of power density with removal efficiencies of 30–87% for COD, 3–84% for total nitrogen (TN), and 8–71% for total phosphorus (TP), during the leachate treatment. Multiple regression analysis of the entire data set revealed that HRT and C_0 had a favorable effect on the removal rates of COD ($R_{rate,COD}$) and TN ($R_{rate,TN}$). TP removal rate ($R_{rate,TP}$) was found to be positively influenced by initial TP concentration ($C_{0,TP}$) but negatively influenced by HRT. In terms of electricity generation, HRT, followed by coulombic efficiency (CE), $R_{rate,COD}$, initial COD concentration ($C_{0,COD}$), internal resistance (R_{in}), and $R_{rate,TP}$ were identified as significant elements whose increase could boost power density production. The MFC performance was found to be consistent and reproducible under similar operating conditions.

Keywords: microbial fuel cell; hydraulic retention time; initial substrate concentration; nutrient removal; COD removal; multiple regression analysis

1. INTRODUCTION

The microbial fuel cell (MFC) is a promising technology that can generate power while wastewater is being biologically treated (Sukkasem, 2011; Klaisongkram & Holasut, 2015; Siripratuma & Pengchai, 2022). A typical MFC comprises anodic and cathodic compartments. In the anodic chamber, microorganisms oxidize organic fuel, such as wastewater, and release electrons and protons throughout their metabolism (Mongkulphit et al., 2021a).

The released electrons that were successfully transferred to an electrode (anode) then transfer to a different electrode (cathode) at the cathodic compartment via an external electrical circuit (Mongkulphit et al., 2021a). Protons that have been discharged will meanwhile diffuse from an anolyte (and may pass through a proton exchange membrane) into the cathodic compartment. A reduction reaction then takes place between the electrons, protons, and oxygen atoms in the cathodic compartment, resulting in the creation of water molecules (Mongkulphit et al., 2021a).

In general, four processes influence MFC performance: 1) the breakdown of the substrate in the anode compartment by microorganisms, 2) the transport of electrons from the microorganisms to the anode electrode, 3) the process of transporting protons from the anode to the cathode, and 4) the reduction of electron acceptors in the cathode compartment (Ye et al., 2019). It is well-known that these 4 processes are affected by the organic loading rate (OLR), which can be calculated using Equation 1, where C_0 represents the initial substrate condition, Q represents the substrate feeding rate, and V_r represents the reactor working volume (Ye et al., 2019).

$$OLR = C_0 \cdot Q / V_r \qquad (1)$$

According to prior studies, the impact of OLR on MFC performance is complex. Increasing the substrate removal and power output of MFCs requires more than merely increasing or decreasing the OLR. For instance, Tamilarasan et al. (2017) found that a continuous up-flow MFC operating in the OLR range of 0.7–3.8 gCOD/L·d obtained the highest COD removal efficiency (78.8%) and maximum power density (116.03 mW/m^2 or 2.2 W/m^3) at the OLR of 1.9 gCOD/L·d. Increased OLR may offer electrogenic bacteria more substrate (Ye et al., 2019), which might then drive a faster rate of substrate removal and, ultimately, lead to higher power output. But if the OLR rose over the optimum value (in this case, 1.9 gCOD/L·d), the extra substrate might act as a niche for methanogens, and methanogenesis might then be foreseen (He et al., 2005). Because methanogens and exoelectrogens actively compete for their substrate at the anode, the performance of MFCs is drastically reduced (Chae et al., 2010). As a result, low removal efficiency and low power output may occur with high OLR. Furthermore, reducing HRT is commonly done to increase OLR. As a result of a higher OLR, the contact time for substrate degradation may be insufficient for saturation microbial activity, decreasing the MFC's ability to produce power (Tamilarasan et al., 2017) and remove waste. Ye et al. (2019) demonstrated that the optimal OLR for substrate removal can be obtained within a certain range. They discovered that at an OLR range of 435–725 mgCOD/L·d, MFC removed over 90% of COD from municipal wastewater, whereas the efficiency of COD removal was reduced to around 70% when the OLR became too high (i.e., 870 mgCOD/L·d). This finding is related to the claim of Molognoni et al. (2016) that substrate limiting constraints can result in high carbon removal efficiencies. It was interesting to note that the experiment of Ye et al. (2019) obtained its maximum power density (253.84 mW/m^2) at the lowest OLR of 435 mgCOD/L·d. A higher anode chamber OLR may increase the danger of membrane fouling (Elakkiya & Matheswaran, 2013), and an accumulation of volatile fatty acid (lactic acid, acetic acid, formic acid, and succinic acid) up to 1,820 mg/L may not facilitate electricity generation in the dual-component MFC (He et al., 2015). Multiple effects of HRT, Q, and C_0 at the same OLR value could lead to this complex OLR influence on the MFC's power output. Previous studies (Min & Logan, 2004; You et al., 2006; Zhao et al., 2014; Kim et al., 2015) have discovered that the maximum PD of MFC and OLR followed the Lineweaver-Burk equation. However, the individual effects of HRT and C_0 on the measured power density (rather than the maximum value) remain unknown.

In terms of substrate removal, the modified Stover-Kincannon model is a well-known kinetic model for analyzing kinetic parameters of biofilm reactors such as rotating biological contactors, trickling filters, and up-flow anaerobic filters (Rajagopal et al., 2013; Sonwani et al., 2019). The modified Stover-Kincannon model (Rajagopal et al., 2013; Sonwani et al., 2019; Nor Faekah et al., 2020) requires experimental data collected at varied OLR to reflect the substrate consumption rate as a function of OLR at steady state. Although OLR might be changed by modifying Q, V_r, or C_0, most studies have been conducted by changing Q in conjunction with changing HRT (Rajagopal et al., 2013; Sonwani et al., 2019; Nor Faekah et al., 2020; Swain et al., 2021). As far as we know, published work evaluating the modified Stover-Kincannon kinetic parameters by varying C_0 is rare. Furthermore, there are very few researchers who vary HRT by adjusting the reactor volume with constant Q. In our previous study, we adjusted Q (15–35 L/d) and V_r while keeping the HRT constant (5 h) and discovered that increasing Q improved both substrate removal rate and power output (Mongkulphit et al., 2021a). The increasing shear rate, which corresponded to the increasing flow rate, was considered to be the most essential factor in enriching biomass and inducing electrogenic activity in an anode chamber (Mongkulphit et al., 2021a). As a result, Q may influence the substrate removal rate as well as the HRT, which is typically recommended to be long enough to allow for saturation microbial activity (He et al., 2005; Greenman et al., 2009). Therefore, if the shift in OLR in the experiment is set up by reducing Q, which coincides with rising HRT, contrasting effects on substrate removal may occur. This may provide a possible explanation for the experiment conducted by Ye et al. (2019), in which comparable COD removal efficiencies (90–96%) were observed under varied HRTs (0.3–0.69 day) and diverse OLRs (43–870 mgCOD/L·d). Therefore, rather than combining Q, C_0, and HRT into a single parameter known as OLR, each of these components should be understood independently for better comprehension.

The aim of this study was to determine the individual effects of HRT and C_0 on MFC performance, based on the hypothesis that HRT and C_0 might be utilized independently to explain the MFCs' substrate removal and power production. In this work, 6 up-flow MFCs were used under 2 different operating conditions: varied HRT at the same C_0, and different C_0 at the same HRT (5 h). Using different V_r under the same Q of 35 L/d allowed the effect of Q to be discounted from both cases. Because MFCs are infrequently utilized for nutrient removal (Ye et al., 2019), total nitrogen (TN) and total phosphorus (TP) were included in the treatment scope, in addition to COD. The experimental data in both scenarios were subjected to multiple regression and the modified Stover-Kincannon model. The wastewater used in this study's treatment phase was a synthetic landfill leachate. Despite the fact that landfill leachate is one of the most difficult substrates to treat (Alkalay et al., 1998), numerous studies have shown that MFCs are effective in removing COD and producing electricity from it (You et al., 2006; Gálvez et al., 2009; Greenman et al., 2009; Puig et al., 2011). In a number of studies, MFCs have been used to treat landfill leachate, yielding very high-power outputs of 2,060.2–6,817.4 mW/m^3, 13,746 mW/m^3, and 20,000 mW/m^3 (Alkalay et al., 1998; You et al., 2006; Gálvez et al., 2009; Zhao et al.,

2014; Puig et al., 2011; Kim et al., 2015; Vazquez-Larios et al., 2015). If the effects of HRT and C_0 on MFC for the treatment of landfill leachate are known individually, a greater improvement in MFC performance should be anticipated.

2. MATERIALS AND METHODS

2.1 MFCs construction
Using a 5.08-cm diameter PVC pipe, 6 membrane-less MFC units with varied anode chamber sizes were constructed (Figure 1). An anode chamber in the base of each MFC was filled with media made from bunches of nylon ropes to obtain the effective 75% void ratio (Mongkulphit et al, 2021b) of the filter bed inside the anode chamber. The filter beds had heights of 0.53 m and volumes (media volume + pore volume) of 3.12 + 1.04 L for MFC1, 0.71 m and 4.17 + 1.39 L for MFC2, 0.88 m and 5.21 + 1.74 L for MFC3, 1.06 m and 6.25 + 2.08 L for MFC4, 1.24 m and 7.29 + 2.43 L for MFC5, and 1.42 m and 8.33 + 2.78 L for MFC6. Each MFC had a top-mounted cathode compartment that contained an air cathode without a separator. Each anode chamber had a triangle-shaped graphite plate serving as the anode, which had 5.2 cm² projected surface area. An elliptical graphite plate cathode with a projected surface area of 20.78 cm² was installed in each MFC as the cathode. To avoid water contact that might trigger a reaction between copper and water, each electrode was attached to a copper cable that was then hot glued shut.
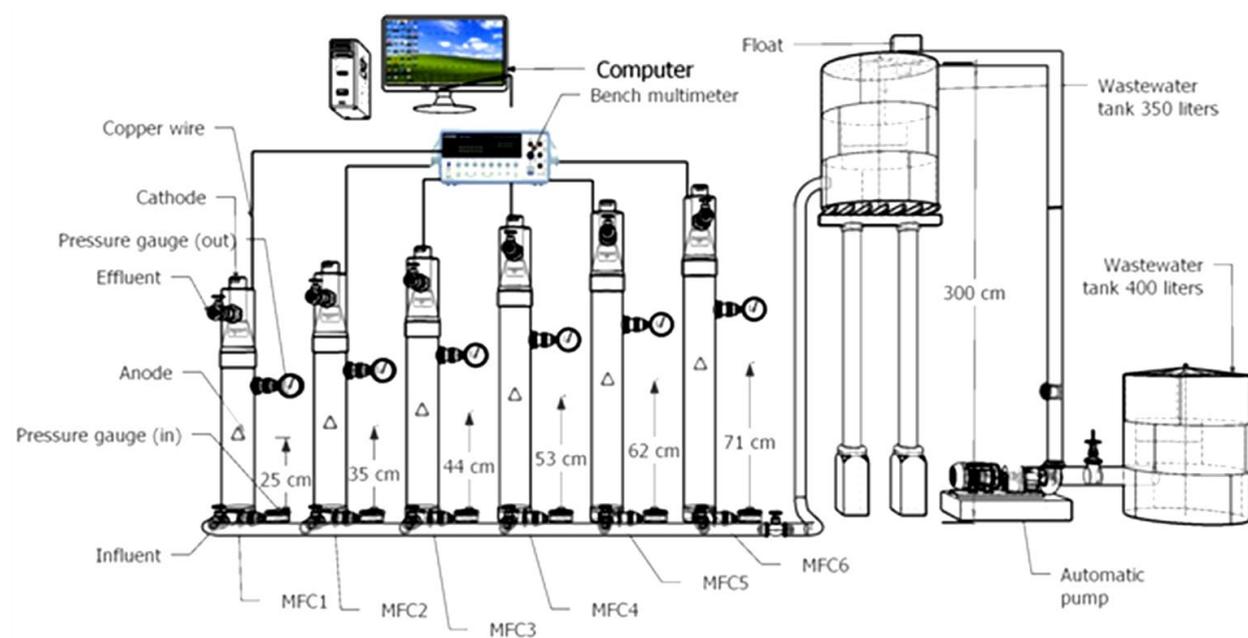

Figure 1. Configuration of up-flow MFCs used in this study

2.2 Synthetic landfill leachate
To prepare synthetic landfill leachate to be utilized in treatment procedures, the following compounds were dissolved in tap water at specific concentrations: acetic acid (CH_3COOH) 0.538 mL/L (5,637 mg/L), propionic acid ($C_3H_6O_2$) 0.385 mL/L (3,785 mg/L), $MgSO_4$, 221.7 mg/L $CaCl_2$, 24.92 mg/L Na_2CO_3, 184.6 mg/L $(COONH_4)_2H_2O$, 110.8 mg/L NaCl, and 0.076 mL/L trans metals solution (TMS) (Halim et al., 2011). TMS was prepared by mixing the following chemicals in one liter of tap water: $CuCl_2$ 0.04 g, $(NH_4)_2SO_4$-$NiSO_4$-H_2O 0.50 g, $(NH_4)_2Fe(SO_4)_2$ H_2O 2 g, $BaCl_2$ 0.05 g, $MnSO_4$ 0.5 g and 96% H_2SO_4 1 mL [26]. Before introducing the synthetic landfill leachate to MFCs, the pH was adjusted to 7–8 by adding NaOH solution (Halim et al., 2011).

2.3 Inoculation and experimental operation
During an inoculation period, each media bed in the anode compartment was immersed for 36 days in a mixture of photosynthetic bacteria derived from Nongpling municipal landfill leachate (Mahasarakham, Thailand) and Siam Rhodo PB liquid fertilizer. The high substrate concentration anolyte (COD 15,755.9 mg/L, BOD 550.0 mg/L, TN 74.0 mg/L, TP 45.1 mg/L, nitrate 6.7 mg/L, nitrite 4.6 mg/L, total ammonia nitrogen 16.6 mg/L, phosphate 5.6 mg/L, pH 9.4) was then circulated for 23 days to enrich the microorganism on the anode and in the filter media. The performance of 6 MFCs was monitored throughout a 23-day recirculating period to validate the presence of electrogenic organisms and their capacity for treatment. The electrical potential of each MFC without the connection to external resistance (OCV: open circuit voltage) was measured using a real-time multimeter (GDM-8255A, Good Will Instrument Co., Ltd.).

Two experiments were performed during the experimental operation period. In the first experiment, synthetic landfill leachate was continuously fed into each MFC for 30 days with the same substrate content and constant Q (35 L/d). This performance provided HRT durations of 2.14 h for MFC1, 2.86 h for MFC2, 3.57 h for MFC3, 4.29 h for MFC4, 5 h for MFC5, and 5.71 h for MFC6. The influent and effluent of each MFC was collected and analyzed for 7 water quality parameters in order to evaluate wastewater treatment performance. Equation 2 and Equation 3 were used to determine the pollutant removal rates (R_{rate}, mg/L·h) and removal efficiencies

(R_{eff}, %) of the MFCs, where C_0 is the parameter concentration in the influent, and C is the parameter concentration in the effluent. A multimeter was used to continuously monitor the voltages for each MFC during the period in order to evaluate the performance of the energy producing system. The MFCs were operated in an open circuit mode with constant Q and particular HRTs (see Table 1) from day 1 to 14 of the treatment period. After that, the first polarization experiment was performed to determine the suitable external resistance (R_{ex}) for each MFC. From days 15 to 20, the MFCs were operated in closed circuit mode by connecting the anode and cathode of each MFC to the appropriate external resistor. On day 20, a second polarization experiment was conducted to reevaluate the acceptable external resistance. Thereafter, the MFCs were run in closed circuit mode until day 30. Q and HRTs were maintained at their pre-period values (see Table 1) throughout the first experiment. Voltage measured in the close circuit condition (day 20–30) was defined as closed circuit voltage (CCV, V). Equation 4 was used to calculate the power density (PD, mW/m^2) generated by the MFCs during closed circuit operation. Aanode is the projected area of an anode.

$$R_{rate} = (C_0 - C)/HRT \qquad (2)$$

$$R_{eff} = (C_0 - C)\ 100/C_0 \qquad (3)$$

$$PD = CCV^2/(R_{ex} \cdot A_{anode}) \qquad (4)$$

For the second experiment, only the MFC5 with the 1.24 m filter bed height was used. To create 6 levels of initial substrate concentration ($C_{0,1}$–$C_{0,6}$, see Table 1), 6 dilution ratios of synthetic landfill leachate were used. Then, one by one, at each concentration level, the synthetic landfill leachate was fed to the MFC at a rate of 35 L/d. In this experiment, the HRT was maintained at 5 hours. At each level of substrate concentration, the MFC was performed for 14 days. Open circuit mode was used for the first seven-day operation. The polarization test was conducted on the 7th day. The chosen Rex was then connected to both MFC electrodes in order to establish closed circuit conditions for the next seven-day operation (day 8–14). The MFC's ability to treat wastewater and generate electricity was investigated during the experiment. After the second experiment, the nylon media of each MFC was randomly collected and analyzed for aerobic and anaerobic plate counts of the adherent biofilm using an in-house method based on FDA-BAM (2001). According to Table 1, the aerobic plate count to anaerobic plate count ratios in MFC1-MFC6 were 0.60, 0.43, 1.28, 2.38, 0.76, and 0.31, respectively. Different HRT could cause differences in microbial populations, which could have an impact on MFC performance.

Table 1. Operation conditions of the first and second experiments

1st experiment	Filter-bed	MFC1	MFC2	MFC3	MFC4	MFC5	MFC6
	Heights (m)	0.53	0.71	0.88	1.06	1.24	1.42
	Media volume (L)	3.12	4.17	5.21	6.25	7.29	8.33
	Pore volume (L)	1.04	1.39	1.74	2.08	2.43	2.78
	HRT (h)	2.14	2.86	3.57	4.29	5	5.71
	Aerobic plate count (CFU/swap)*	6.6×10^5	3.8×10^5	9.7×10^5	6.2×10^5	1.3×10^5	1.1×10^6
	Anaerobic plate count (CFU/swap area)*	1.1×10^6	8.7×10^5	7.6×10^5	2.6×10^5	1.7×10^5	3.6×10^6
	Q (L/d)	35					
	C_0 COD (mg/L)	$1,214.6 \pm 127.3$					
	TN (mg/L)	53.3 ± 8.6					
	TP (mg/L)	50.4 ± 10.3					
2nd experiment	Operation conditions	$C_{0,1}$	$C_{0,2}$	$C_{0,3}$	$C_{0,4}$	$C_{0,5}$	$C_{0,6}$
	COD (mg/L)	573.9 ± 56.8	1095.7 ± 237.6	2087.2 ± 165.7	3219.8 ± 457.7	4318.3 ± 239.9	4913.5 ± 136.1
	TN (mg/L)	9.2 ± 1.4	30.1 ± 6.8	39.4 ± 1.9	52.9 ± 7.3	86.0 ± 3.5	113.7 ± 6.6
	TP (mg/L)	3.6 ± 0.3	23.9 ± 5.2	34.4 ± 1.6	41.4 ± 2.8	60.1 ± 4.9	74.5 ± 2.6
	Q (L/d)	35					
	HRT (h)	5**					

Note: Q: flow rate, HRT: hydraulic retention time, C_0: initial concentration, COD: chemical oxygen demand, TN: total nitrogen, TP: total phosphorus, * At the end of the experiment, the aerobic and anaerobic plate counts of biofilm adhering to the nylon media were measured using an in-house method based on FDA-BAM (2001), ** MFC5 was chosen for the 2nd experiment

2.4 Polarization experiment
A polarization experiment was carried out for each MFC at the end of OCV monitoring and on day 20 of the initial experiment. The CCVs across each Rex were measured and used to compute the PDs transmitted to the R_{ex} after connecting the anode and cathode of each MFC to various external resistances (20,000, 10,000, 7,500, 2,200, 1,000, 560, 250, 150, and 10 ohms) for 5 min each. The R_{ex} with the highest PD for each MFC was considered appropriate and then used in the closed circuit MFC treatment process.

2.5 Water quality analytical method
The influent and effluent from each MFC were collected and analyzed for COD using the closed-reflux titrimetric method (Method 5220 C (APHA, 2016)); total nitrogen

(TN) using the alkaline peroxodisulfate digestion method (Gou, 2001); and TP using the sulfuric acid–nitric acid digestion method (Methods 4500-P (APHA, 2016)) throughout the incubation and treatment periods. The influent and effluent samples' oxidation-reduction potential (ORP), dissolved oxygen (DO), and pH levels were also assessed using ORP, DO, and pH meters.

2.6 Internal resistance

The R_{in} (ohm) of each MFC was calculated by entering data from CCV, OCV, and I (electrical current (A) under the prescribed load determined as I = CCV/R_{ex}) into Equation 5 (Ieropoulos et al., 2008).

$$R_{in} = (OCV/I) - R_{ex} \qquad (5)$$

2.7 Coulombic efficiency

The Coulombic efficiency (CE, %), which represents the recovery of electrons, was calculated using Equation 6, where t is the MFC's operating time, F (C/mol), is the Faraday's constant at 96485, V is the total porosity volume of the filter bed in the anode chamber, and Δ COD (mg/L), is the difference in COD concentrations between the influent and effluent of the MFC (Logan, 2007).

$$CE = (8\int_0^t Idt) \times 100 \,/\, F\Delta CODV \qquad (6)$$

2.8 Stover-Kincannon plot of Michaelis-Menten kinetics

In order to perform a kinetic analysis of the pollutant removal rate, the Stover-Kincannon plot of the Michaelis-Menten kinetics, as shown in Equation 7 (Borghei et al., 2008), was used to plot the 1/R_{rate} of each pollutant, such as COD, TN, or TP, with the 1/OLR. The Michaelis-Menten constant (kB) and the highest achievable removal rate ($R_{rate-max}$) were determined using linear regression analysis to get the coefficients of Equation 7.

$$1/R_{rate} = ((kB/R_{rate-max})(1/OLR)) + (1/R_{rate-max}) \qquad (7)$$

2.9 Multiple regression analysis

Using SPSS software (IBM SPSS Statistics 25), experimental parameters were analyzed by multiple regression analysis to determine the effects of HRT and C_0 on MFC performance.

3. RESULTS AND DISCUSSION

3.1 Performance of the MFCs

3.1.1 Wastewater treatment performance

During the inoculation period, it was demonstrated that all MFCs removed COD at specific efficiencies (27.17±20.72% for MFC1; 11.08±7.73% for MFC2; 21.32±12.14% for MFC3; 21.74±26.23% for MFC4; 25.33±21.40% for MFC5; and 36.24±47.74% for MFC6) and produced a certain OCV (0.18±0.02V for MFC1; 0.24±0.02V for MFC2; 0.30±0.02V

for MFC3; 0.167±0.04V for MFC4; 0.35±0.04V for MFC5; and 0.22±0.01V for MFC6).

During the treatment period, MFCs' anode chambers were operated at a pH range of 7.00 to 8.68, with a DO concentration of 1.33 to 1.75 mg/L, and an ORP range of -422 to -105 mV. No adverse pH effect should occur in the treatment effectiveness of the MFCs because a pH of 6.5–8.5 is typically advised for biological treatment (Englande et al., 2015). It is well known that DO inhibits denitrification and anaerobic ammonium oxidation (anammox) processes (Lie & Welander, 1994). When anammox and partial denitrification were combined, the DO had to be maintained at or below 0.7 mg/L (You et al., 2020). According to Campos et al. (2015), a nitrogen removal rate of 600 mg/L/d was recorded at both DO concentrations of 1 and 8 mg/L, even though oxygen could completely penetrate the bacterial cells in the granular biomass at the latter DO dosage. Additionally, an ORP lower than the range of -50 to +50 mV, which is known to be favorable for denitrification, was discovered in the experiment of Kumar & Lin (2010). As a result, although very unlikely, there is still a chance in this study that TN could be eliminated through the denitrification and anammox processes. For TP removal, the DO and ORP conditions employed in this study did not typically support the phosphate releasing and accumulating processes of the phosphorus-accumulating organisms (PAOs). The DO concentrations in our MFCs did not meet the recommended range of 0.0 to 0.2 mg/L for the phosphorus releasing process (Shehab et al., 1996). The anolyte had negative ORP values. While this was suitable for the phosphorus-releasing process, it was outside the recommended range for the PAO's during phosphate-accumulation, which should occur at positive ORP values in aerobic conditions. Therefore, PAOs shouldn't be the main phosphorus remover in this system.

In the first experiment, all MFCs could remove COD, TN, and TP from the influent when HRT was varied from 2.14 to 5.71 h at the same starting substrate concentrations, as shown in Figure 2. With a R_{eff} of 9.24–77.67%, COD was reduced from 1,030.63–1,412.34 mg/L to 282.04–1,150.74 mg/L with a R_{eff} of 4.35–73.22%; TN decreased from 43.92–66.83 mg/L to 15.5–48.25 mg/L with a R_{eff} of 4.21–87.21%; and TP decreased from 33.22–63.56 mg/L to 4.25–50.71 mg/L with a R_{eff} of 15.74–67.16%. MFC6, which had the longest HRT, also had the highest R_{eff}. This discovery indicated that the required contact time for wastewater treatment reaction was at least 5.71 h.

To assess the precision of MFCs' ability to treat wastewater in the first experiment, three data points with similar influent concentrations were chosen and the average effluent concentrations and standard deviations were determined (see Table 2). Because the standard deviation of the effluent ranged from 1.97 to 28.78% for COD concentration, 0.36 to 3.09% for TN concentration, and 3.71 to 10.91% for TP concentration, the results from the first experiment are considered to have a considerable degree of repeatability.
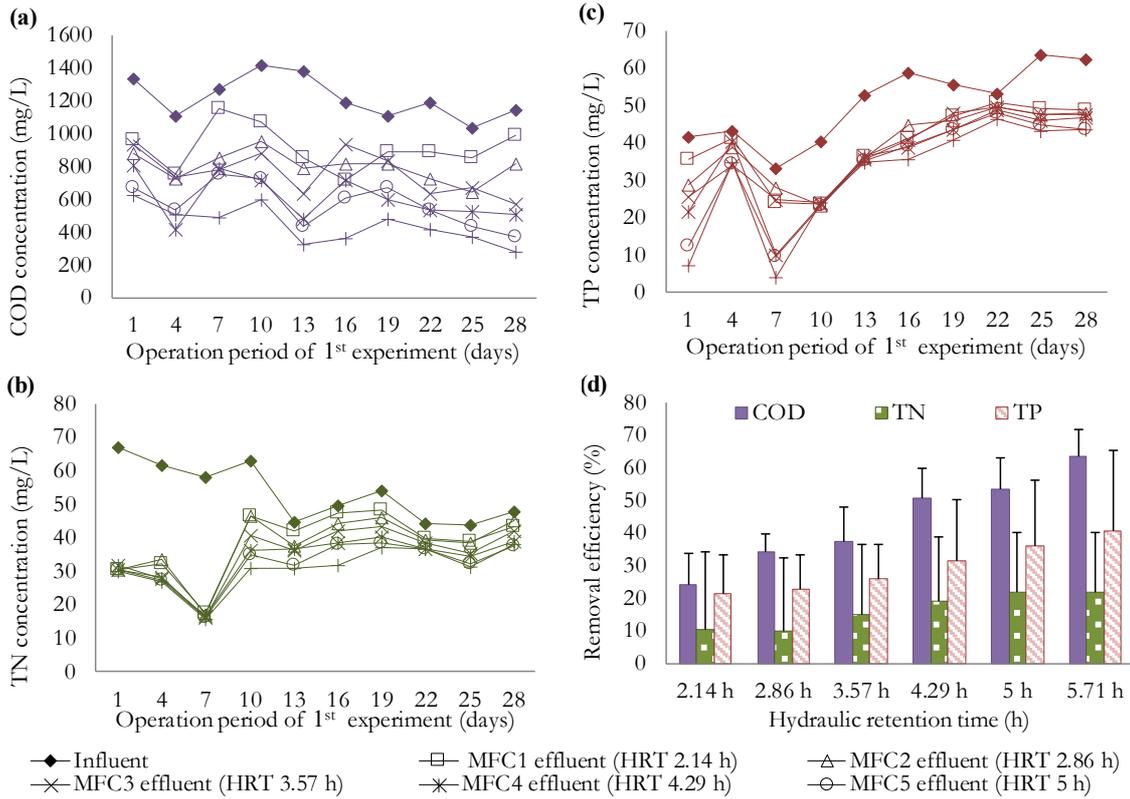
Figure 2. Synthetic landfill leachate treatment and removal efficiencies of MFCs in the first experiment; (a) chemical oxygen demand (COD) concentrations, (b) total nitrogen (TN) concentrations, (c) total phosphorus (TP) concentrations, and (d) average removal efficiencies

Table 2. The precision of MFCs' ability to treat wastewater in the first experiment

Parameter		Data 1 (day)	Data 2 (day)	Data 3 (day)	Average	Standard deviation (%*)
Influent	COD (mg/L)	1,106.97 (day 4)	1,106.97 (day 19)	1,145.14 (day 28)	1,119.70	22.04 (1.97%)
	TN (mg/L)	49.53 (day 16)	53.78 (day 19)	47.71 (day 28)	151.02	3.11 (2.06%)
	TP (mg/L)	58.86 (day 16)	63.56 (day 25)	62.44 (day 28)	61.62	2.46 (3.98%)
Effluent	MFC1 COD (mg/L)	748.16	890.67	983.30	874.04	118.45 (13.55%)
	MFC1 TN (mg/L)	47.38	48.25	43.46	139.10	2.55 (1.83%)
	MFC1 TP (mg/L)	41.27	49.20	48.54	46.33	4.40 (9.50%)
	MFC2 COD (mg/L)	723.01	817.32	817.32	785.88	54.45 (6.93%)
	MFC2 TN (mg/L)	44.10	46.04	44.85	134.98	0.98 (0.73%)
	MFC2 TP (mg/L)	44.76	47.53	47.96	46.75	1.74 (3.71%)
	MFC3 COD (mg/L)	734.80	835.00	567.80	712.53	134.98 (18.94%)
	MFC3 TN (mg/L)	41.88	43.17	42.01	127.06	0.71 (0.56%)
	MFC3 TP (mg/L)	40.81	47.50	47.41	45.24	3.84 (8.48%)
	MFC4 COD (mg/L)	415.64	593.78	504.71	504.71	89.07 (17.65%)
	MFC4 TN (mg/L)	38.57	40.02	38.79	117.38	0.78 (0.66%)
	MFC4 TP (mg/L)	38.95	46.12	46.69	43.92	4.31 (9.81%)
	MFC5 COD (mg/L)	534.40	668.00	367.40	523.27	150.61 (28.78%)
	MFC5 TN (mg/L)	38.00	38.42	37.59	114.00	0.41 (0.36%)
	MFC5 TP (mg/L)	39.19	44.60	43.67	42.49	2.89 (6.81%)
	MFC6 COD (mg/L)	504.71	475.02	282.04	420.59	120.90 (28.75%)
	MFC6 TN (mg/L)	31.77	36.99	37.86	106.62	3.23 (3.09%)
	MFC6 TP (mg/L)	35.66	43.25	43.48	40.80	4.45 (10.91%)

Note: *: The standard deviation of the average value in percentage units was calculated by dividing it by the average value and multiplying that figure by 100

Figure 3 illustrates the removal of COD, TN, and TP in the second experiment when the C_0s were changed at the same HRT (5 h). The COD concentrations dropped from 184.02–4,822.17 mg/L to 106.67–3,217.01 mg/L with removal efficiencies of 30.03–87.02%. The removal efficiency of TN was 2.91–84.49% as it decreased from 7.32–124.11 mg/L to 3.85–84.21 mg/L. With removal efficiencies of 8.04–70.77%, TP decreased from 3.20–78.32 mg/L to 1.10–57.77 mg/L. The maximum removal efficiencies for COD, TN, and TP were obtained by the initial concentrations of $C_{0,3}$ (COD 1,892.17–2,245.97 mg/L, TN 37.31–41.38 mg/L, and TP 33.10–36.17 mg/L). This is in accordance with the theory that increasing C_0 may provide electrogenic bacteria with more substrate, which would increase the substrate removal rate, but that too much C_0 might provide methanogens a place to grow, which would significantly reduce MFC performance (Chae et al., 2010). Because the DO condition in our experiment did not enable traditional biological nutrient removal, the most likely pathway for removing TN and TP in this study could be chemical precipitation at the cathode compartment. At 2.0 mg/L DO, Tao et al. (2014) reported that more than 85% of TN and more than 90% of TP were removed from their synthetic wastewater. Their precipitate investigation revealed that phosphate, carbonate, and hydroxyl compound precipitates occurred in their cathode chamber (Tao et al., 2014). To verify this hypothesis, additional analysis will be required in future research.

To evaluate the precision of MFCs' ability to treat wastewater in the second experiment, the standard deviation of effluent water quality (error bars of the bar graph in Figure 3) could be used. As the standard deviation ranged from 11.8 to 13.8% for COD concentration in $C_{0,5}$ and $C_{0,6}$, 3.6 to 11.8% for TN concentration in $C_{0,4}$, $C_{0,5}$, and $C_{0,6}$, and 2.6 to 14.2% for TP concentration in $C_{0,3}$, $C_{0,4}$, $C_{0,5}$, and $C_{0,6}$, it can be determined that the second experiment achieved a considerable level of repeatability at high initial concentrations.
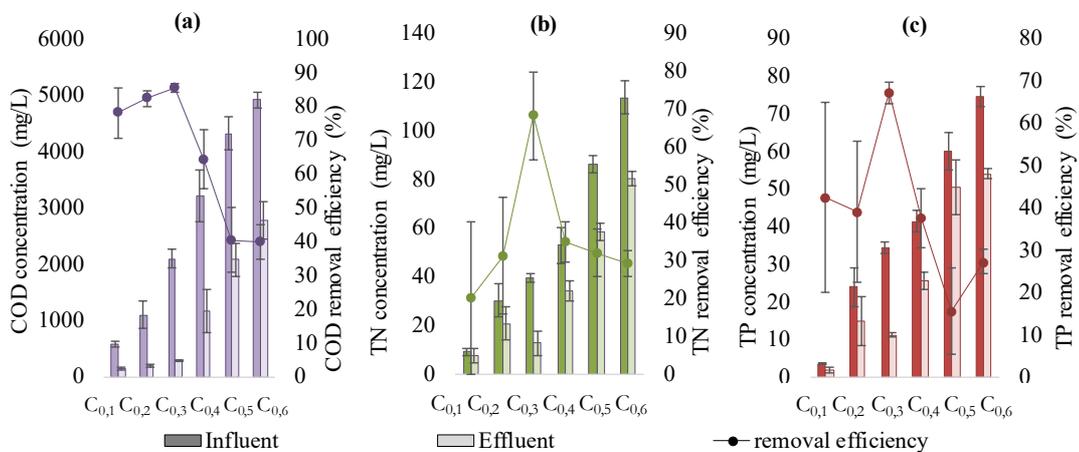

Figure 3. Synthetic landfill leachate treatment and removal efficiencies of the MFC in the second experiment; (a) chemical oxygen demand (COD), (b) total nitrogen (TN), (c) total phosphorus (TP)

3.2 Electricity generation performance

Figures 4(a) and 4(b) show the voltages and power densities during the first experiment. MFCs were operated in an open circuit with an OCV ranging from 0.06 to 0.83 V from the 1st to the 14th day. The first polarization experiment, performed at the end of day 14, and the second polarization experiment, performed at the end of day 20, both suggested that 7,500 ohms was the appropriate external resistance for all MFCs. The electricity performance of the MFCs was monitored until day 30 by connecting the anode and cathode of each MFC to the 7,500 Ω external resistor. The results of CCV and PD monitoring from days 15 to 30 revealed that the HRT for the largest power generation was 5 h (0.38–0.83 V, 37–80 mW/m²), followed by 4.29 h (0.27–0.65 V, 19–34 mW/m²), 5.71 h (0.24–0.63 V, 5–30 mW/m²), 3.57 h (0.13–0.58 V, 4–31 mW/m²), 2.14-h HRT (0.06–0.41 V, 1–16 mW/m²) and 2.86-h HRT (0.07–0.58 V, 1–11 mW/m²), respectively. The excessive electrode distance could be one potential explanation for why the longest HRT in this study, 5.71 h with constant Q and C_0, did not provide the highest power density. Larger HRT was associated with a longer distance between the anode and cathode of each reactor due to the architecture of our MFC reactors. As a result, long HRT (5.71 h, for example) can cause protons and electrons to travel farther than they should, which could ultimately result in a low power output. Furthermore, because the MFCs were membraneless, electrodes placed too close together may allow electrons to shortcut directly from the anode chamber to the cathode chamber via the flowing influent. This could have been the cause of the poor power density at 2.14 and 2.86 hours of HRT.

Figures 4(c) and 4(d) show the electrical results of the second experiment. An MFC achieved the highest PD (38.00–47.76 mW/m²) and the highest CCV (0.313–0.679 V) with a medium range of substrate concentration level, $C_{0,4}$ (COD = 3219.84 ± 457.72 mg/L, TN = 52.87±7.27 mg/L, TP = 41.38 ± 2.83 mg/L). The lowest PD (5.89–13.21 mW/m²) and lowest CCV (0.283–0.588 V) were produced by the MFC at $C_{0,2}$ level (COD = 1,095.67 ± 237.58 mg/L, TN = 30.11 ± 6.84 mg/L, TP = 23.94 ± 5.19 mg/L). For $C_{0,1}$, the lowest substrate concentration (COD = 573.91 ± 56.76 mg/L, TN = 9.20 ± 1.39 mg/L, and TP = 3.62 ± 0.29 mg/L), the MFC only produced a high PD (55.08 ± 16.78 mW/m²) on the 8th day before dropping to 10.71–13.51 mW/m² during the 10th to the 14th day. The beneficial impact of low phosphate concentration and the devastating effect of low COD concentration are two aspects reported in earlier literature that can be used to explain this finding. According to Yanuka-Golub

et al. (2016), MFCs operating at lower phosphate concentrations (16 mg/L) were able to reach peak voltage more quickly than those operating at higher phosphate concentrations (134 mg/L), likely as a consequence of a faster colonization of anode-respiring bacteria (bacteria that can donate electrons to an anode as their terminal electron acceptor). As a result, on the first day of CCV monitoring, a significant PD could be observed in the $C_{0,1}$ condition. However, if the colonization of anode-respiring bacteria had achieved its maximum level by the end of day 8, the beneficial effects of low

phosphate concentration on power density should not have continued past that point. According to Sun et al. (2019), the ideal substrate concentration might encourage the growth of the electrochemically active biofilm, which in turn enhances the anodic redox processes. Therefore, as the microorganisms continued to develop (after day 8), the lowest COD content in the $C_{0,1}$ condition could have resulted in substrate depletion, which would have had a negative impact on power generation. After the 8th day, this could have caused the voltage and power output at $C_{0,1}$ level to decline.
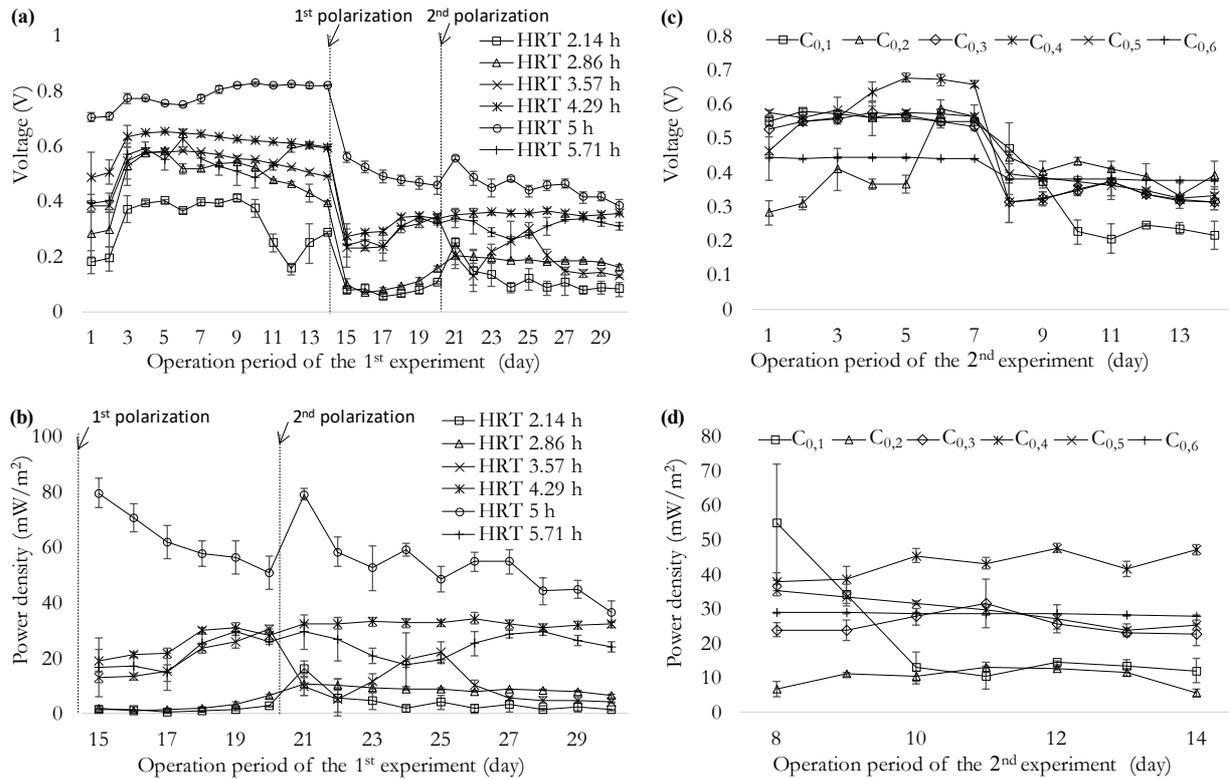

Figure 4. Average voltages and power densities of MFCs; (a) voltage, (b) power density in the first experiment, and (c) voltage, (d) power density in the second experiment

To precisely determine the power generation capacity of MFCs, the average PDs and their standard deviations were computed. In the first experiment, the mean PD data ± standard deviation from day 15 to day 20 (after the first polarization) and from day 21 to day 30 (after the second polarization) were 1.65 mW/m² ± 45.25% and 4.41 mW/m² ± 101.15% for MFC1; 2.86 mW/m² ± 67.03% and 8.92 mW/m² ± 13.40% for MFC2; 20.42 mW/m² ± 36.81% and 9.86 mW/m² ± 65.18% for MFC3; 25.35 mW/m² ± 20.01% and 32.62 mW/m² ± 2.48% for MFC4; 62.93 mW/m² ± 16.60% and 53.37 mW/m² ± 21.47% for MFC5; and 21.67 mW/m² ± 28.25% and 25.00 mW/m² ± 16.84% for MFC6. The repeatability of MFCs with long HRT (MFC4-MFC6) appears to have been higher than that of MFCs with short HRT (MFC1-MFC3). In the second experiment, the mean PD data ± standard deviation was 21.86 mW/m² ± 76.40% for $C_{0,1}$; 10.32 mW/m² ± 27.58% for $C_{0,2}$; 25.54 mW/m² ± 12.65% for $C_{0,3}$; 43.11 mW/m² ± 9.06% for $C_{0,4}$; 29.58 mW/m² ± 14.41% for $C_{0,5}$; and 28.67 mW/m² ± 1.22% for $C_{0,6}$. Compared to MFCs with low initial

concentrations ($C_{0,1}$, $C_{0,2}$), those with high initial concentrations ($C_{0,3}$, $C_{0,4}$, $C_{0,5}$, $C_{0,6}$) had higher PD generation reproducibility.

Figure 5 displays the CE and R_{in} of the MFCs in both experiments. As the HRT (Figure 5(a)) or C_0 (Figure 5(b)) increased, a declining trend in CE was observed. This finding contrasted with the trend of COD removal efficiency, which rose as a result of the increasing HRTs. Non-electrogenic bacteria may have dominated COD digesters under longer HRT or higher C_0 conditions, making it difficult for them to transfer electrons to extracellular electron acceptors. A similar explanation was offered by Zhang et al. (2015) for their finding that the CEs of their MFC were greater for the lower initial COD, under both 1000-R_{ex} and 100-R_{ex}. A declining trend in R_{in} was observed because of the increase in HRT. One possible explanation is that because the electrode distance and HRT of the MFCs in this study correlated with reactor volume, an MFC with a larger reactor volume would also have a longer HRT and electrode distance. Also, because a longer

electrode distance prevents electrons from traveling directly from an anode to a cathode (shortcut moving), an immense flow of electrons across the electrical wire is anticipated in the case of a large reactor volume. The internal resistance may therefore have decreased as

reactor volume was increased. At the $C_{0,2}$ and $C_{0,6}$ levels of substrate concentration, low R_{in} values were found. The maximal power output, however, was not attained at $C_{0,2}$ or $C_{0,6}$. This indicated the presence of additional important variables, such as CE, $R_{rate,COD}$, and $C_{0,COD}$.
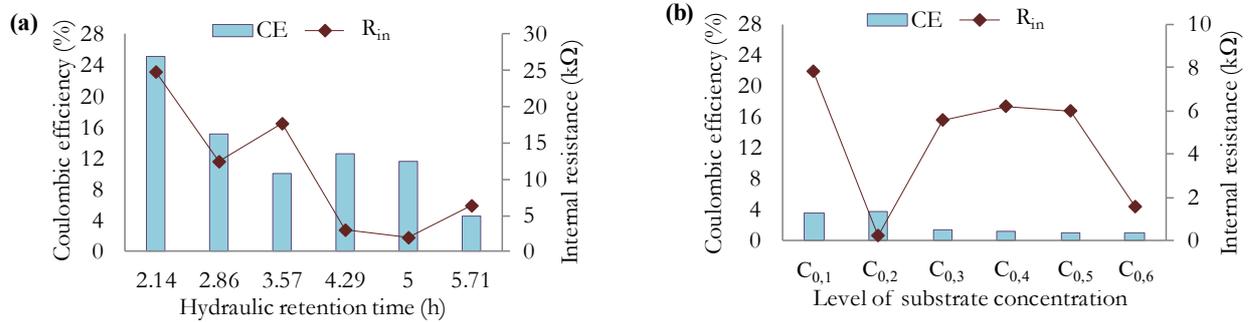

Figure 5. Coulombic efficiency (CE) and internal resistance (Rin) in the experiments; (a) the first experiment, and (b) the second experiment

3.3 Roles of HRT and initial substrate concentration in wastewater treatment

Identical OLR values did not result in the same level of COD removal efficiencies in separate experiments. Due to changes in HRT and initial COD concentration ($C_{0,COD}$), the influence of the same OLR range on the trend of COD removal rate ($R_{rate,COD}$) varied. As shown in Figure 6(a), when the HRT changed from 2.1 to 5.7 h with a constant $C_{0,COD}$ (1410.4 mg/L) in the first experiment, the COD removal efficiency ($R_{eff,COD}$) decreased as a result of the rise in OLR. In contrast, in the second experiment (HRT = 5 h, $C_{0,COD}$ = 573.9–4,832.2 mg/L), the $R_{rate,COD}$ increased as a result of the rise in OLR. The same pattern was also seen for the COD removal rate ($R_{rate,COD}$) (see Figure 6(b)). According to this finding, $C_{0,COD}$ should be considered as a separate parameter because it can have an opposite impact on COD removal from the HRT.

Multiple regression analysis was carried out to identify important variables affecting $R_{eff,COD}$ in order to provide more insight (see Table 3). The variables utilized in the analysis were in the form of both general values and inverted values (1/ $R_{eff,COD}$, 1/HRT, 1/$C_{0,COD}$). The shaded row of the $R_{eff,COD}$ model in Table 3, which had the highest determination coefficient (r^2 = 0.83), was utilized to discuss $R_{eff,COD}$ enhancement in more detail. Standardized coefficients of the model (0.842 for HRT and -0.625 for $C_{0,COD}$) significantly demonstrated the favorable impact of the HRT (p = 0.0003) and the adverse impact of the $C_{0,COD}$ (p = 0.002) on $R_{eff,COD}$. These results suggests that $C_{0,COD}$, and HRT should be separated into distinct parameters rather than integrating them into one parameter, OLR. This finding may be explained by the $R_{eff,COD}$ -calculation approach, which divides the removed COD concentration by the $C_{0,COD}$. The calculating equation may cause the $R_{eff,COD}$ to be lower when the $C_{0,COD}$ concentration is significantly higher than the removed COD concentration.

However, the outcome differed when we focused on the $R_{rate,COD}$ regression model. The shaded row for $R_{rate,COD}$ in Table 3 was chosen for the discussion of $R_{rate,COD}$ improvement because it had the highest r^2 (0.97). The

model's standardized coefficients showed that both the $C_{0,COD}$ and HRT had significantly similar beneficial impacts on the $R_{rate,COD}$ (1/HRT: standardized coefficient = 0.702, coefficients standard error = 0.002, p = 0.0000007; 1/$C_{0,COD}$: standardized coefficient = 0.662, coefficients standard error = 0.0004, p = 0.000001). As the standard errors of the coefficients were 8% for 1/HRT and 1/$C_{0,COD}$, such impacts were considered fairly precise. Furthermore, the results reveal that the Michaelis-Menten kinetics model's traditional Stover-Kincannon plot (the model denoted by an asterisk in Table 2) was unable to adequately describe $R_{rate,COD}$ in this investigation. In terms of nutrient removal, contrast impact also appeared within the same range of substrate loading rate. As demonstrated in Figures 6(c) and 6(d), the first experiment's declining TN and TP loading rates were accompanied by decreasing TN and TP removal rates ($R_{rate,TN}$ and $R_{rate,TP}$). Contrarily, in the second experiment, $R_{rate,TN}$ and $R_{rate,TP}$ increased as a result of the corresponding increase in TN and TP loading rates.

The multiple regression models in Table 4 with the greatest r^2 values (0.844, 0.886; the shaded rows) were utilized to discuss the improvement of $R_{rate,TN}$ and $R_{rate,TP}$. Both $R_{rate,TN}$ and $R_{rate,TP}$ (p = 0.05) rose considerably as a result of the rise in the initial concentrations of TN and TP ($C_{0,TN}$, and $C_{0,TP}$). The standardized coefficients of the shaded rows in Table 4 show that increasing $C_{0,TN}$ (standardized coefficient = 0.926, coefficients standard error = 1.716 (14%), p = 0.00006) and $C_{0,TP}$ (standardized coefficient = 0.928, coefficients standard error = 1.137 (12.3%), p = 0.00002) significantly increased TN and TP removal rates. According to the coefficients of 1/ HRT in TN and TP regression equations, increasing HRT may have had little positive impact on the $R_{rate,TN}$ while having a minor negative impact on the $R_{rate,TP}$. However, these coefficients' p-values (0.346, 0.616) were more than 0.05, hence these effects were regarded as insignificant. It should be observed that the traditional Stover-Kincannon plot of the Michaelis-Menten kinetics model could well explain the $R_{rate,TP}$ (r^2 = 0.885), but poorly explain the $R_{rate,TN}$ (r^2 = 0.600) in this work.
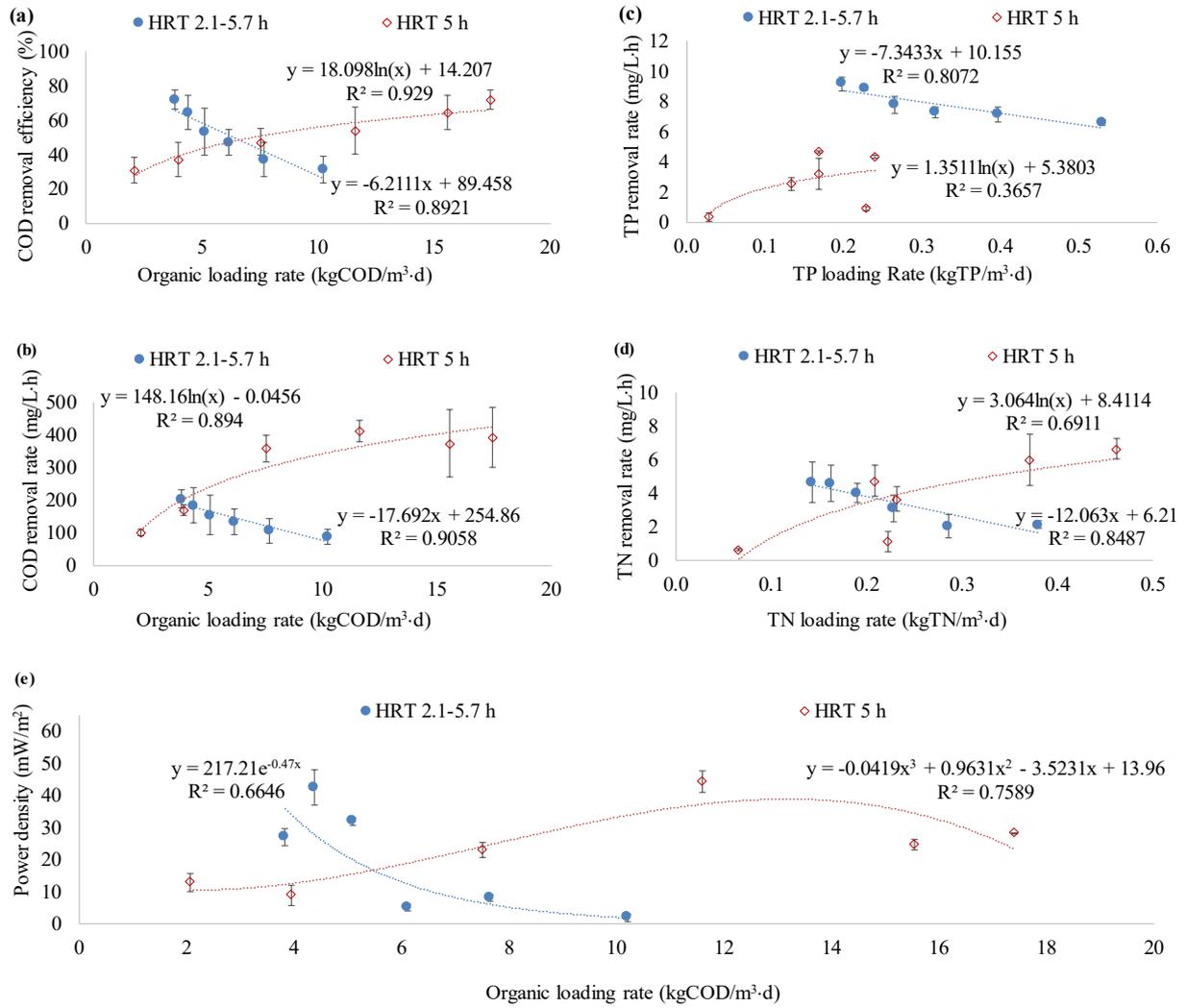
Figure 6. Relationship between organic loading rate and pollutant removal; (a) COD removal efficiency, (b) COD removal rate, (c) TN removal rate, (d) TP removal rate) and (e) power density

Table 3. Linear multiple regression analysis for the estimation of COD removal

Response variable	Explanatory variables	Unstandardized coefficients	Standardized coefficients	Coefficients standard error	*p*-value
$R_{eff, COD}$	Constant	8.697	-	11.625	0.473
($r^2 = 0.830$)	HRT	15.173	0.842	2.618	0.0003
	$C_{0, COD}$	-0.0089	-0.625	0.002	0.002
$1/ R_{eff, COD}$	Constant	0.009	-	0.003	0.026
($r^2 = 0.800$)	$1/ HRT$	0.062	0.815	0.011	0.0003
	$1/ C_{0, COD}$	-0.007	-0.415	0.002	0.019
$R_{rate, COD}$	Constant	-103.996	-	69.786	0.170
($r^2 = 0.85$)	HRT	40.813	0.350	15.716	0.029
	$C_{0, COD}$	0.070	0.765	0.012	0.000
$1/ R_{rate, COD}$*	Constant	-0.004	-	0.001	0.0002
($r^2 = 0.970$)	$1/ HRT$	0.025	0.702	0.002	0.0000007
	$1/ C_{0, COD}$	0.005	0.662	0.0004	0.000001
$1/ R_{rate, COD}$	Constant	0.004	-	0.002	0.031
($r^2 = 0.184$)**	$1/ OLR$	0.011	0.429	0.007	0.164

Note: COD: chemical oxygen demand, $R_{eff, COD}$: COD removal efficiency, $R_{rate, COD}$: COD removal rate, $C_{0, COD}$: initial COD concentration, *: the proposed model for considering $R_{rate, COD}$, r^2: determination coefficient, *p*-value: the level of marginal significance within the hypothesis testing, **: conventional Stover-Kincannon plot of Michaelis-Menten kinetics model

Table 4. Linear multiple regression analysis for the estimation of TN and TP removal

Response variable	Explanatory variables	Unstandardized coefficients	Standardized coefficients	Coefficients standard error	*p*-value
$R_{rate, TN}$	Constant	0.610	-	0.744	0.431
(r^2 = 0.668)	$C_{0, TN}$	0.059	0.817	0.013	0.001
1/ $R_{rate, TN}$	Constant	0.088	-	0.072	0.248
(r^2 = 0.827)	$1/C_{0, TN}$	11.775	0.910	1.702	0.000041
1/ $R_{rate, TN}$*	Constant	-0.072	-	0.176	0.694
(r^2 = 0.844)	1/HRT	0.635	0.132	0.638	0.346
	$1/ C_{0, TN}$	11.985	0.926	1.716	0.00006
1/ $R_{rate, TN}$	Constant	-0.049	-	0.148	0.748
(r^2 = 0.600)**	1/TN loading rate	0.093	0.775	0.024	0.003
$R_{rate, TP}$	Constant	0.797	-	1.875	0.680
(r^2 = 0.394)	$C_{0, TP}$	0.086	0.628	0.034	0.029
1/ $R_{rate, TP}$	Constant	0.084	-	0.095	0.398
(r^2 = 0.883)	$1/C_{0, TP}$	9.331	0.939	1.076	0.000006
1/ $R_{rate, TP}$	Constant	0.224	-	0.286	0.455
(r^2 = 0.886)	1/HRT	-0.557	-0.059	1.072	0.616
	$1/C_{0, TP}$	9.222	0.928	1.137	0.00002
1/ $R_{rate, TP}$	Constant	-0.094	-	0.106	0.395
(r^2 = 0.885)*	1/TP loading rate	0.084	0.941	0.010	0.000005

Note: TN: total nitrogen, TP: total phosphorus, $R_{rate, TN}$: TN removal rate, $R_{rate, TP}$: TP removal rate, $C_{0, TN}$: initial TN concentration, $C_{0, TP}$: initial TP concentration, *: the proposed equation for considering $R_{rate, TN}$ and $R_{rate, TP}$, r^2: determination coefficient, *p*-value: the level of marginal significance within the hypothesis testing, **: Conventional Stover-Kincannon plot of Michaelis-Menten kinetics model

3.4 Roles of HRT and initial substrate concentration in electricity generation

Figure 6(e) shows the effect of OLR on average PD. The first experiment's decrease in OLR led to a trend in PD values that was similar to the trend of $R_{rate,COD}$ (Figure 6(b)). In the second experiment, however, the PD fluctuated erratically and peaked at 44.33 mW/m² at 11.59 gCOD/m³·d OLR. This finding suggests that instead of considering OLR as the sole key input element for PD estimate, HRT and $C_{0,COD}$ should be taken into account independently.

Table 5. Linear multiple regression analysis for the estimation of power density output

Response variable	Explanatory variables	Unstandardized coefficients	Standardized coefficients	Coefficients standard error	*p*-value
Average *PD*	Constant	-277.577	-	25.429	0.008
(r^2 = 0.999)	log(HRT)	339.309	2.997	47.724	0.019
	CE	4.539	2.387	0.108	0.001
	$R_{rate,COD}$	0.146	1.269	0.004	0.001
	$1/vol._{anode}$	33.232	0.606	1.036	0.014
	$C_{0,COD}$	0.006	0.603	0.000	0.006
	$R_{rate,TP}$	0.734	0.154	0.152	0.040
	log(e-distance)	-275.297	-1.183	86.513	0.086
	$R_{rate,TN}$	-7.446	-0.972	0.339	0.002
	$1/R_{in}$	-3.257	-0.326	0.145	0.002

Note: PD: power density, $R_{rate, COD}$: COD removal rate, $R_{rate, TN}$: TN removal rate, $R_{rate, TP}$: TP removal rate, $C_{0, COD}$: initial COD concentration, CE: coulombic efficiency, R_{in}: internal resistance, e-distance: electrode distance, vol. $_{anode}$: anodic working volume, r^2: determination coefficient, *p*-value: the level of marginal significance within the hypothesis testing

The parameters affecting the PD output were identified using multiple regression analysis. Table 5 shows that 8 parameters had a substantial impact on PD formation (*p* = 0.001–0.040). It may be concluded from positive standardized coefficients that the PD increases as CE, $R_{rate,COD}$, $C_{0,COD}$, and $R_{rate,TP}$ increase. However, prolonging HRT, which corresponds to an increase in log (HRT) (standardized coefficient = 2.997, coefficients standard error = 47.724 (14.1%), *p* = 0.019), should be the most efficient method of raising the PD. It was discovered that the inverse of anodic working volume ($1/vol._{anode}$) had a beneficial effect on PD production (standardized coefficient = 0.606, coefficients standard error = 1.036 (3.1%), *p* = 0.014). In order to achieve high PD output, it is therefore preferable to reduce the anodic working volume since this could result in better mixing conditions. In Table 5, $R_{rate,TN}$, and $1/R_{in}$ were shown to have negative effects on the generation of PD with a negative standardized coefficient (*p* = 0.002). The mechanism for the removal of TN, such as chemical precipitates, may reduce the quantity of electron transfer from an anode to anolyte. Consequently, the PD dropped at a greater $R_{rate,TN}$. This

study makes the claim that higher R_{in} could considerably increase PD output. In general, this result is implausible. The highest PD, however, is achieved when the total R_{ex} and total R_{in} of the power source are equal (Pinto et al., 2011). Therefore, higher PD isn't usually the result of lower R_{in}. There may not be enough electrons available to discharge outside the cell in the case of MFCs that produce relatively low direct current. A scarcity of accessible electrons will result from too low R_{in}, which will allow too many extra electrons to flow out of the MFC. Therefore, in this instance, the R_{in} needs to be high enough to prevent an electron shortage, give adequate CCV, and maintain I, all of which will lead to a high and consistent PD output. To consistently maintain the maximum PD, real-time measurement of the MFC's R_{in} and real-time modification of R_{ex} are necessary. The results shown in Table 5 for the electrode distance (e-distance) factor reveal that a shorter e-distance would likely encourage a greater PD value. However, the trend was not significant ($p = 0.086$).

4. CONCLUSION

Basic experiments were conducted to investigate the performance of up-flow MFCs and to examine the influence of individual parameters, namely HRT and C_0. At 6 different HRTs (the first experiment) and 6 different C_0 conditions (the second experiment), the treatment of synthetic landfill leachate and the production of electricity by the up-flow MFCs were investigated. According to the experimental data, the highest PD (79.14 mW/m²) was observed in the first experiment at 5-h HRT, 1,106.97-mg/L $C_{0,COD}$, and 4.0-kgCOD/m³·d COD loading rate, while the highest removal efficiencies of COD (85.55±1.15%), TN (68.28± 11.60%), and TP (67.16±2.68%) were observed in the second experiment at 5-h HRT, 2087.22±165.66-mg/L $C_{0,COD}$, 34.40±1.55-mg/L $C_{0,TN}$, 39.42±1.93-mg/L $C_{0,TP}$, and 7.5-kgCOD/m³·d COD loading rate. Based on multiple regression analysis, the outcome strongly suggests that HRT and $C_{0,COD}$ have a favorable impact on the $R_{rate,COD}$. In the case of nutrient removal, increasing $C_{0,TN}$ and $C_{0,TP}$ significantly increased $R_{rate,TN}$ and $R_{rate,TP}$, respectively. In terms of electricity generation, HRT, CE, $R_{rate,COD}$, $C_{0,COD}$, R_{in}, and $R_{rate,TP}$ were identified as significant factors that positively influenced PD production. In contrast, $R_{rate,TN}$, and vol.$_{anode}$ were found to have negative impacts on PD output. Although the reactor design is not novel and there is no analysis of electrogenic bacteria in the biofilm, this study has proven the hypothesis that HRT and C_0 can be used separately to explain MFC substrate removal and power generation.

ACKNOWLEDGMENTS

REFERENCES

Alkalay, D., Guerrero, L., Lema, J. M., Mendez, R., & Chamy, R. (1998). Review: Anaerobic treatment of municipal sanitary landfill leachates: The problem of refractory and toxic components. *World Journal of Microbiology and Biotechnology*, *14*(3), 309–320. https://doi.org/10.1023/A:1008876107787

APHA (2016). *Standard methods for the examination of water and wastewater* (20th ed.). American Public Health Association. https://www.pdfdrive.com/standard-methods-for-the-examination-of-water-and-wastewater-e11311928.html

Borghei, S. M., Sharbatmaleki, M., Pourrezaie, P., & Borghei, G. (2008). Kinetics of organic removal in fixed-bed aerobic biological reactor. *Bioresource Technology*, *99*(5), 1118–1124. https://doi.org/10.1016/j.biortech.2007.02.037

Chae, K. J., Choi, M. J., Kim, K. Y., Ajayi, F. F., Park, W., Kim, C. W., & Kim, I. S. (2010). Methanogenesis control by employing various environmental stress conditions in two-chambered microbial fuel cells. *Bioresource Technology*, *101*(14), 5350–5357. https://doi.org/10.1016/j.biortech.2010.02.035

Campos, J. L., Méndez, R., & Mosquera-Corral, A. (2015). Influence of dissolved oxygen concentration on the start-up of the anammox-based process: ELAN®. *Water Science & Technology*, *72*(4), 520–527. https://doi.org/10.2166/wst.2015.233

Elakkiya, E., & Matheswaran, M. (2013). Comparison of anodic metabolisms in bioelectricity production during treatment of dairy wastewater in microbial fuel cell. *Bioresource Technology*, *136*, 407–412. https://doi.org/10.1016/j.biortech.2013.02.113

Englande, A. J. Jr., Krenkel, P., & Shamas, J. (2015). Wastewater treatment & water reclamation. *Reference Module in Earth Systems and Environmental Sciences*, *2023*, 639–670. https://doi.org/10.1016/B978-0-12-409548-9.09508-7

Gálvez, A., Greenman, J., & Ieropoulos, I. (2009). Landfill leachate treatment with microbial fuel cells; scale-up through plurality. *Bioresource Technology*, *100*(21), 5085–5091. https://doi.org/10.1016/j.biortech.2009.05.061

Gou, Y. (2001). Determination of total nitrogen in water samples by spectrophotometry using phenol after alkaline peroxodisulfate digestion. *Bunseki Kagaku*, *50*(7), 481–486. https://doi.org/10.2116/bunsekikagaku.50.481

Greenman, J., Galvez, A., Giusti, L., & Ieropoulos, I. (2009). Electricity from landfill leachate using microbial fuel cells: Comparison with a biological aerated filter. *Enzyme and Microbial Technology*, *44*(2), 112–119. https://doi.org/10.1016/j.enzmictec.2008.09.012

Halim, A. A., Abidin, Z., Nazurah, N., Normah, A., Anuar, I., Othman, S. M., & Mohd, I. W. (2011). Ammonia and COD removal from synthetic leachate using rice husk composite adsorbent. *Journal of Urban and Environmental Engineering*, *5*(1), 24–31. https://doi.org/10.4090/juee.2011.v5n1.024031

He, Z., Minteer, S. D., & Angenent, L. T. (2005) Electricity generation from artificial wastewater using an upflow microbial fuel cell. *Environmental Science & Technology*, *39*(14), 5262–5267. https://doi.org/10.1021/es0502876

He, Y., Liu, Z., Xing, X. H., Li, B., Zhang, Y., Shen, R., Zhu, Z., & Duan, N. (2015). Carbon nanotubes simultaneously as

the anode and microbial carrier for up-flow fixed-bed microbial fuel cell. *Biochemical Engineering Journal*, *94*, 39–44. https:// doi.org/10.1016/j.bej.2014.11.006

Ieropoulos, I., Greenman J., & Melhuish, C. (2008). Microbial fuel cells based on carbon veil electrodes: Stack configuration and scalability. *International Journal of Energy Research*, *32*(13), 1228–1240. https://doi.org/10.1002/er.1419

Kim, H., Kim, B., & Yu, J. (2015). Power generation response to readily biodegradable COD in single-chamber microbial fuel cells. *Bioresource Technology*, *186*, 136–140. https://doi.org/10.1016/j.biortech.2015.03.066

Klaisongkram, N., & Holasut, K. (2015). Electricity generation of plant microbial fuel cell (PMFC) using Cyperus involucratus R. *Engineering and Applied Science Research*, *42*(1), 117–124. https://doi.org/10.14456/kkuenj.2015.2

Kumar, M., & Lin, J. G. (2010). Co-existence of anammox and denitrification for simultaneous nitrogen and carbon removal-Strategies and issues. *Journal of Hazardous Materials*, *178*(1-3), 1–9. https://doi.org/10.1016/j.jhazmat.2010.01.077

Lie, E., & Welander, T. (1994). Influence of dissolved oxygen and oxidation-reduction potential on the denitrification rate of activated sludge. *Water Science & Technology*, *30*(6), 91–100. https://doi.org/10.2166/wst.1994.0256

Logan, B. E. (2007). *Microbial fuel cells*, (2nd ed.). John Wiley & Sons.

Min, B., & Logan, B. E. (2004). Continuous electricity generation from domestic wastewater and organic substrates in a flat plate microbial fuel cell. *Environmental Science & Technology, 38*(21), 5809–5814. https://doi.org/10.1021/es0491026

Molognoni, D., Puig, S., Balaguer, M. D., Capodaglio, A. G., Callegari, A., & Colprim, J. (2016). Multiparametric control for enhanced biofilm selection in microbial fuel cells. *Journal of Chemical Technology & Biotechnology*, *91*(6), 1720–1727. https://doi.org/10.1002/jctb.4760

Mongkulphit, S., Pengchai, P., & Suwannata, N. (2021a). Influence of very high flow rates on performance of biofilter-microbial fuel cells. *International Journal of Environmental Science and Development*, *12*(3), 69–74. https://doi.org/10.18178/ijesd.2021.12.3.1320

Mongkulphit, S., Siripratum, S., Chumroen, W., & Pengchai, P. (2021b). Roles of packed bed porosity on performance of biofilter microbial fuel cell in synthetic landfill leachate treatment. *GMSARN International Journal*, *15*(4), 360–365.

Nor Faekah, I., Fatihah, S., & Mohamed, Z. S. (2020). Kinetic evaluation of a partially packed upflow anaerobic fixed film reactor treating low-strength synthetic rubber wastewater. *Heliyon*, *6*(3), Article e03594. https://doi.org/10.1016/j.heliyon.2020.e03594

Pinto, R. P., Srinivasan, B., Guiot, S. R., & Tartakovsky, B. (2011). The effect of real-time external resistance optimization on microbial fuel cell performance. *Water Research*, *45*(4), 1571–1578. https://doi.org/10.1016/j.watres.2010.11.033

Puig, S., Serra, M., Coma, M., Cabré, M., Balaguer, M. D., & Colprim, J. (2011). Microbial fuel cell application in landfill leachate treatment. *Journal of Hazardous Materials*, *185*(2-3), 763–767. https://doi.org/10.1016/j.jhazmat.2010.09.086

Rajagopal, R., Torrijos, M., Kumar, P., & Mehrotra, I. (2013). Substrate removal kinetics in high-rate upflow anaerobic filters packed with low-density polyethylene media treating high-strength agro-food wastewaters. *Journal of Environmental Management*, *116*, 101–106. https://doi.org/10.1016/j.jenvman.2012.11.032

Siripratuma, S., & Pengchai, P. (2022). Performance investigation of the reverse anoxic/anaerobic/oxic microbial fuel cell. *Engineering Journal*, *26*(10), 11–25. https://doi.org/10.4186/ej.2022.26.10.11

Shehab, O., Deininger, R., Porta, F., & Wojewski, T. (1996). Optimizing phosphorus removal at the Ann Arbor wastewater treatment plant. *Water Science & Technology*, *34*(1-2), 493–499. https://doi.org/10.1016/0273-1223(96)00548-3

Sonwani, R. K., Swain, G., Giri, B. S., Singh, R. S., & Rai, B. N. (2019). A novel comparative study of modified carriers in moving bed biofilm reactor for the treatment of wastewater: Process optimization and kinetic study. *Bioresource Technology*, *281*, 335–342. https://doi.org/10.1016/j.biortech.2019.02.121

Sukkasem, C. (2011). Microbial fuel cell: Novel technology "convert wastewater to electricity". *Engineering and Applied Science Research*, *38*(3), 347–362.

Sun, G., Kang, K., Qiu, L., Guo, X., & Zhu, M. (2019). Electrochemical performance and microbial community analysis in air cathode microbial fuel cells fuelled with pyroligneous liquor. *Bioelectrochemistry*, *126*, 12–19. https://doi.org/10.1016/j.bioelechem.2018.11.006

Swain, G., Singh, S., Sonwani, R. K., Singh, R. S., Jaiswal, R. P., & Rai, B. N. (2021). Removal of acid orange 7 dye in a packed bed bioreactor: Process optimization using response surface methodology and kinetic study. *Bioresource Technology Reports*, *13*, Article 100620. https://doi.org/10.1016/j.biteb.2020.100620

Tamilarasan, K., Banu, J. R., Jayashree, C., Yogalakshmi, K. N., & Gokulakrishnan, K. (2017). Effect of organic loading rate on electricity generating potential of upflow anaerobic microbial fuel cell treating surgical cotton industry wastewater. *Journal of Environmental Chemical Engineering*, *5*(1), 1021–1026. https://doi.org/10.1016/j.jece.2017.01.025

Tao, Q., Luo, J., Zhou, J., Zhou, S., Liu, G., & Zhang, R. (2014). Effect of dissolved oxygen on nitrogen and phosphorus removal and electricity production in microbial fuel cell. *Bioresource Technology*, *164*, 402–407. https://doi.org/10.1016/j.biortech.2014.05.002

Vazquez-Larios, A. L., Poggi-Varaldo, H. M., Solorza-Feria, O., & Rinderknecht-Seijas, N. (2015). Effect of type of inoculum on microbial fuel cell performance that used RuxMoySez as cathodic catalyst. *International Journal of Hydrogen Energy*, *40*(48), 17402–17412. https://doi.org/10.1016/j.ijhydene.2015.09.143

Yanuka-Golub, K., Reshef, L., Rishpon, J., & Gophna, U. (2016). Community structure dynamics during startup in microbial fuel cells - The effect of phosphate concentrations. *Bioresource Technology*, *212*, 151–159. https://doi.org/10.1016/j.biortech.2016.04.016

Ye, Y., Ngo, H. H., Guo, W., Chang, S. W., Nguyen, D. D., Liu, Y., Nghiem, L. D., Zhang, X., & Wang, J. (2019). Effect of organic loading rate on the recovery of nutrients and energy in a dual-chamber microbial fuel cell. *Bioresource Technology*, *281*(18), 367–373. https://doi.org/10.1016/j.biortech.2019.02.108

You, Q. G., Wang, J. H., Qi, G. X., Zhou, Y. M., Guo, Z. W., Shen, Y., & Gao, X. (2020). Anammox and partial denitrification coupling: A review. *RSC Advances*, *10*(21), 12554–12572. https://doi.org/10.1039/D0RA00001A

You, S. J., Zhao, Q. L., Jiang, J. Q., Zhang, J. N., & Zhao, S. Q. (2006). Sustainable approach for leachate treatment: Electricity generation in microbial fuel cell. *Journal of Environmental Science and Health, 41*(12), 2721–2734. https://doi.org/10.1080/10934520600966284

Zhang, X., He, W., Ren, L., Stager, J., Evans, P. J., & Logan, B. E. (2015). COD removal characteristics in air-cathode microbial fuel cells. *Bioresource Technology*, *176*, 23–31. https://doi.org/10.1016/j.biortech.2014.11.001

Zhao, Y., Ma, Y., Li, T., Bo, X., Wang, J., Li, P., Zhong, L., & Sun, Y. (2014). Treatment of sewage and synchronous electricity generation characteristics by microbial fuel cell. *Journal of Fuel Chemistry and Technology*, *42*(4), 481–486. https://doi.org/10.1016/S1872-5813(14)60024-4.